Electron Acceptor Hot Paper

Deutsche Ausgabe: DOI: 10.1002/ange.201601305
Internationale Ausgabe: DOI: 10.1002/anie.201601305

Polymer Acceptor Based on B←N Units with Enhanced Electron Mobility for Efficient All-Polymer Solar Cells

Ruyan Zhao, Chuandong Dou, Zhiyuan Xie,* Jun Liu,* and Lixiang Wang*

Abstract: *We demonstrate that polymer electron acceptors with excellent all-polymer solar-cell (all-PSC) device performance can be developed from polymer electron donors by using B←N units. By alleviating the steric hindrance effect of the bulky pendant moieties on the conjugated polymers that contain B←N units, the π–π stacking distance of polymer backbones is decreased and the electron mobility is consequently enhanced by nearly two orders of magnitude. As a result, the power conversion efficiency of all-PSCs with the polymer acting as the electron acceptor is greatly improved from 0.12 % to 5.04 %. This PCE value is comparable to that of the best all-PSCs with state-of-the-art polymer acceptors.*

All-polymer solar cells (all-PSCs), which use conjugated polymers as both the electron donor and electron acceptor, have attracted much attention because of their advantages over conventional polymer/fullerene solar cells, including enhanced light absorption and improved stability of the morphology.[1] Great progress has recently been made in developing all-PSCs by selecting polymer donors/acceptors with matched absorption spectra or crystallinity, and by optimizing film-forming conditions.[2] Li and co-workers have demonstrated all-PSCs with a power conversion efficiency (PCE) exceeding 8.0 %, which is comparable to that of polymer/fullerene solar cells.[2a] On the other hand, further development of all-PSCs is severely limited because of the lack of polymer electron acceptors. Efficient polymer electron acceptors must possess both low-lying LUMO and HOMO energy levels ($E_{LUMO/HOMO}$) as well as high electron mobilities (μ_e).[3] To date, only a few specific polymers based on naphthalene diimide (NDI) units, perylene diimide (PDI) units, or double B←N bridged bipyridine (BNBP) units show these essential properties and can work as promising polymer electron acceptors for all-PSC devices.[2–4]

There are many more polymer electron donors than polymer electron acceptors.[5] Yamaguchi and co-workers have developed a novel thienylthiazole skeleton containing B←N units to design electron-transporting small molecules with high electron mobilities.[6] We recently disclosed a strategy to develop polymer electron acceptors from typical polymer electron donors by replacing a C–C unit with a B←N unit.[7,8] Although the resulting polymer **P-BN-TPD** (Figure 1) exhibits a low-lying $E_{LUMO/HOMO}$, its all-PSC device performance is poor because of its low electron mobility.[7] This is attributed to the steric hindrance of the bulky pendant phenyl groups on the B atom, which are necessary for stabilization of tetracoordinated boron compounds but prevent close π stacking of the conjugated polymer backbones.[9,10]

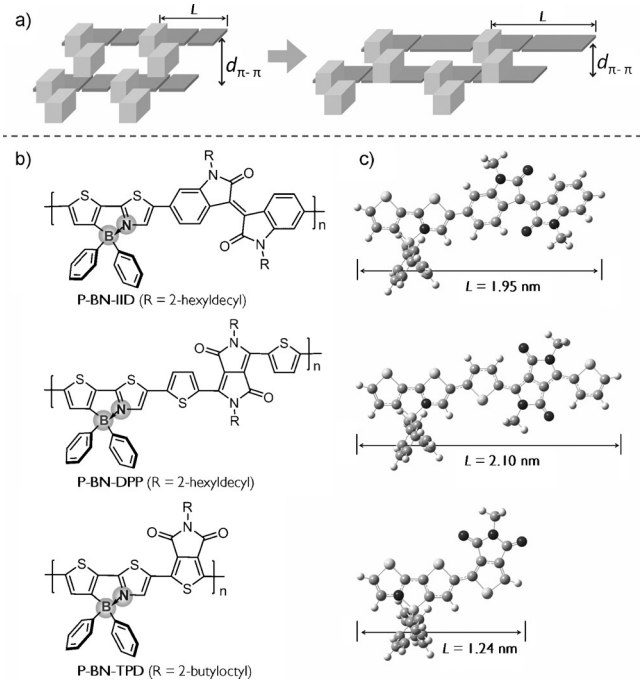

Figure 1. a) Schematic illustration of the approach to decrease the π-stacking distance of polymer backbones by extending the length of repeating units; b) chemical structures of **P-BN-IID**, **P-BN-DPP**, and **P-BN-TPD**; c) the optimized molecular configurations and the lengths of their repeating units. Note that the chemical structures should be regiorandom because of the unsymmetric BNTT unit.

Herein, we extend the lengths of the repeating units of polymer electron acceptors to alleviate the steric hindrance effect of the pendant phenyl groups (Figure 1). The resulting polymer exhibits a decreased π-stacking distance, and consequently shows dramatically enhanced electron mobility and greatly improved all-PSC device performance. Isoindigo (IID) units and dithienyldiketopyrrolopyrrole (DPP) units

[*] R. Zhao, Dr. C. Dou, Prof. Z. Xie, Prof. J. Liu, Prof. L. Wang
State Key Laboratory of Polymer Physics and Chemistry Changchun Institute of Applied Chemistry
Chinese Academy of Sciences
Changchun 130022 (P.R. China)
E-mail: chuandong.dou@ciac.ac.cn
xiezy_n@ciac.ac.cn
liujun@ciac.ac.cn
R. Zhao
University of the Chinese Academy of Sciences
Beijing 100864 (P.R. China)

Supporting information for this article can be found under: http://dx.doi.org/10.1002/anie.201601305.

have been widely used in highly efficient polymer electron donors and are much longer than the previously used thienopyrrolodione (TPD) unit.[11] As shown in Figure 1 two novel polymer electron acceptors, **P-BN-IID** and **P-BN-DPP**, have been developed based on the B←N strategy and using IID units and DPP units. The all-PSC device with **P-BN-IID** as the acceptor and poly[4,8-bis(5-(2-ethylhexyl)thiophen-2-yl)benzo[1,2-*b*:4,5-*b*′] dithiophene-*co*-3-fluorothieno[3,4-*b*]thiophene-2-carboxylate] (PTB7-Th) as the donor shows a power conversion efficiency of 5.04%,[12] which is comparable to that of the best all-PSCs with polymer acceptors based on NDI or PDI units.[2–4] These results indicate that polymer electron acceptors with excellent all-PSC devices performance can be developed from polymer electron donors by using B←N units.

Figure 1b shows the chemical structures of the three polymers, **P-BN-IID**, **P-BN-DPP**, and **P-BN-TPD**. They have alternating B←N bridged thienylthiazole (BNTT) and IID/DPP/TPD units in the conjugated polymer backbones. The BNTT was prepared by the same procedure as used by Yamaguchi and co-workers for its dimesitylboryl analogue.[6] The three polymers were synthesized by Stille polymerization (see the Supporting Information). As the BNTT unit is unsymmetric, these polymers should be regiorandom because both head-to-head and head-to-tail connections of the BNTT unit and the IID/DPP/TPD unit may exist. Gel permeation chromotography (GPC) with 1,2,4-trichlorobenzene as the eluent at 150°C gave a number-average molecular weight (M_n) and polydispersity (PDI) of 18.0 kDa and 2.56 for **P-BN-IID**, 17.0 kDa and 2.35 for **P-BN-DPP**, and 10.1 kDa and 1.88 for **P-BN-TPD**, respectively. All three polymers show good thermal stability, with thermal decomposition temperatures (T_d) of over 280°C.

Geometry optimizations were performed at the B3LYP/6-31G* level of theory to elucidate the configurations of the repeating units in the three polymers (see the Supporting Information).[13] As shown in Figure 1c, the two phenyl groups on the B atom of the BNTT unit adopt a dihedral angle of 75° with the thienylthiazole skeleton, thereby suggesting that the steric bulk of the two phenyl groups prevents stacking of the polymer backbones in the solid state. The lengths of the repeating units of **P-BN-IID**, **P-BN-DPP**, and **P-BN-TPD** are 1.95 nm, 2.10 nm, and 1.24 nm, respectively. The longer repeating units of **P-BN-IID** and **P-BN-DPP** compared to that of **P-BN-TPD** are expected to reduce the steric effect of the pendant phenyl groups. Although the backbones of the repeating units of **P-BN-DPP** and **P-BN-TPD** have fully planar conformations, a twisted conformation is observed for that of **P-BN-IID**, with an optimized twist angle of 24° between the IID and BNTT units. The slightly twisted conformation of **P-BN-IID** is expected to improve the interactions of the polymer backbones despite the presence of bulky groups.

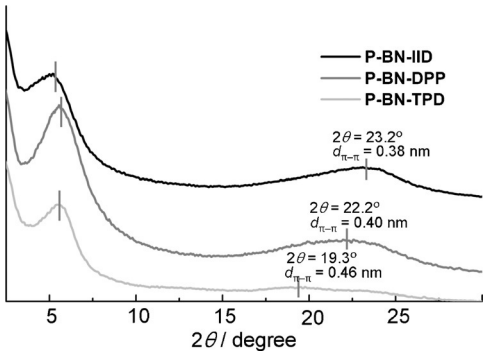

Figure 2. GI-XRD patterns of the drop-cast films of **P-BN-IID**, **P-BN-DPP**, and **P-BN-TPD**.

Figure 2 shows the grazing incident X-ray diffraction (GI-XRD) patterns of drop-cast films of the three polymers. **P-BN-TPD** shows a broad diffraction band at 19.3°, which corresponds to an average π–π stacking distance ($d_{\pi\text{-}\pi}$) of the polymer backbones of 0.46 nm. In comparison, **P-BN-IID** and **P-BN-DPP** exhibit diffraction peaks at 23.2° and 22.2°, which correspond to $d_{\pi\text{-}\pi}$ values of 0.38 nm and 0.40 nm, respectively. Compared with **P-BN-TPD**, **P-BN-IID** and **P-BN-DPP** have smaller $d_{\pi\text{-}\pi}$ values because of their longer repeating units, which significantly alleviates the steric hindrance effect of the pendent phenyl groups. The small $d_{\pi\text{-}\pi}$ value facilitates electron hopping between the polymer backbones, and thus leads to enhanced electron mobility. The electron mobilities of the three polymers were estimated using the space-charge-limited current (SCLC) method together with the current density/voltage (*J*-*V*) curves of the electron-only devices. The electron mobilities of **P-BN-IID**, **P-BN-DPP**, and **P-BN-TPD** are $2.80\times10^{-5}\,cm^2V^{-1}s^{-1}$, $8.48\times10^{-6}\,cm^2V^{-1}s^{-1}$, and $3.40\times10^{-7}\,cm^2V^{-1}s^{-1}$, respectively (Table 1). The electron mobility of **P-BN-IID** is higher than that of **P-BN-TPD** by nearly two orders of magnitude because of the smaller π–π stacking distance.

The absorption spectra of the three polymers in *o*-dichlorobenzene (*o*-DCB) solutions and in thin films are shown in Figure 3a. The absorption spectrum of **P-BN-TPD** in solution shows a narrow band with maxima at 588/557 nm, while the absorption bands of **P-BN-IID** and **P-BN-DPP** in solution are broad and red-shifted with maxima at 690/638 nm and 755 nm, respectively. The absorption spectra of thin films

Table 1: Molecular weights, photophysical and electrochemical properties, and electron mobilities of the three polymers.

Polymer	M_n [kDa]	PDI	λ_{abs}[a] [nm]	ε_{max}[a] [$M^{-1}cm^{-1}$]	λ_{abs}[b] [nm]	E_g^{opt}[b] [eV]	E_{onset}^{ox}[c] [V]	E_{onset}^{red}[c] [V]	E_{HOMO}[d] [eV]	E_{LUMO}[d] [eV]	μ_e [$cm^2V^{-1}s^{-1}$]
P-BN-IID	18.0	2.56	690/638	64000	695/642	1.63	+1.04	−1.0	−5.84	−3.80	2.80×10^{-5}
P-BN-DPP	17.0	2.35	755	76000	761	1.37	+0.52	−1.23	−5.32	−3.57	8.48×10^{-6}
P-BN-TPD	10.1	1.88	588/557	64000	609/566	1.88	+1.05	−1.07	−5.85	−3.73	3.40×10^{-7}

[a] Measured in *o*-DCB solution. [b] Measured in thin film. [c] Onset potential versus Fc/Fc^+. [d] Calculated from: $E_{HOMO/LUMO} = -(4.80 + E_{onset}^{ox}/E_{onset}^{red})$ eV.

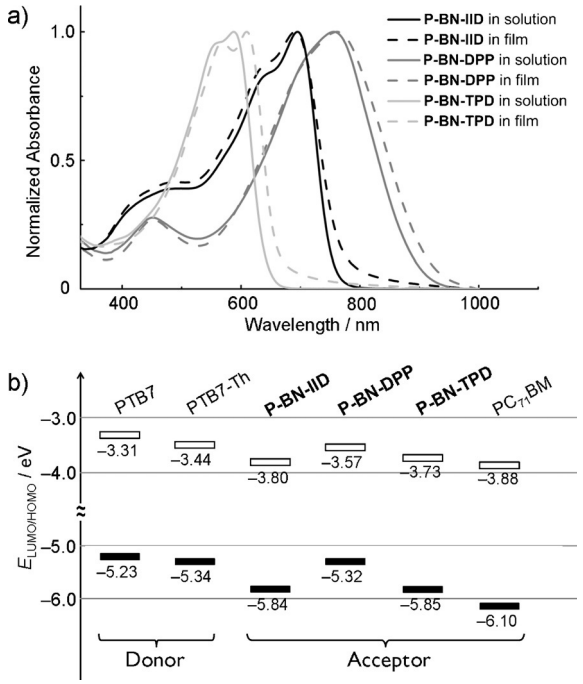

Figure 3. a) UV/Vis absorption spectra of **P-BN-IID**, **P-BN-DPP**, and **P-BN-TPD** in solution and in films; b) schematic representation of the LUMO/HOMO energy level alignments of the polymer donors and the acceptors.

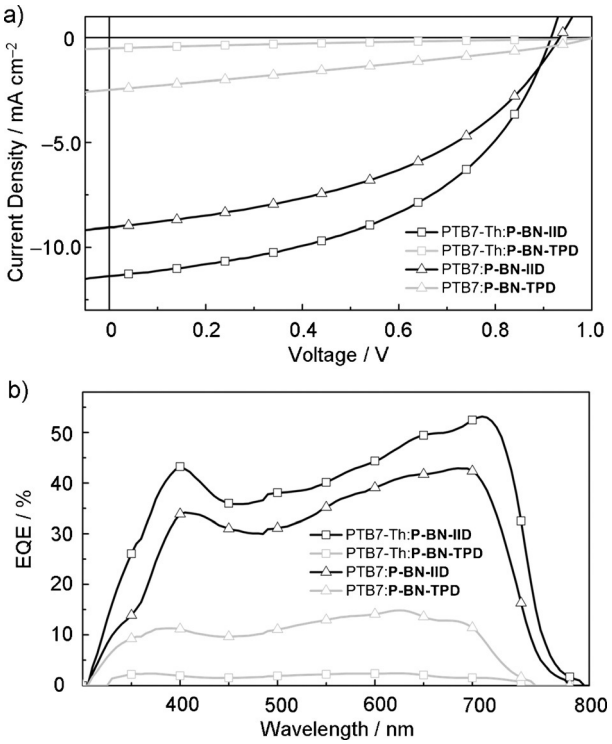

Figure 4. a) *J-V* curves and b) EQE spectra of the all-PSC devices with **P-BN-IID**/**P-BN-TPD** as the electron acceptor and PTB7-Th/PTB7 as the electron donor.

are slightly red-shifted relative to the counterparts in solutions. From the onset absorption wavelength in films, the optical band gaps (E_g) of **P-BN-IID**, **P-BN-DPP**, and **P-BN-TPD** are estimated to be 1.63 eV, 1.37 eV, and 1.88 eV, respectively.

Cyclic voltammetry (CV) measurements were carried out on films of the three polymers to estimate the LUMO/HOMO energy levels of the three polymers (see the Supporting Information). The $E_{LUMO/HOMO}$ values of the three polymers were estimated from the onsets of the reduction and oxidation potentials in the cyclic voltammograms (Table 1). As shown in Figure 3b, the $E_{LUMO/HOMO}$ values of **P-BN-IID** and **P-BN-TPD** are −3.80 eV/−5.84 eV and −3.73 eV/−5.85 eV, respectively, which are comparable to those of [6,6]-phenyl-C71-butyric acid methyl ester ($PC_{71}BM$). The $E_{LUMO/HOMO}$ values of **P-BN-IID** and **P-BN-TPD** match well with those of widely used polymer donors, such as PTB7-Th and poly({4,8-bis[(2-ethylhexyl)oxy]-benzo[1,2-b:4,5-b′]dithiophene-2,6-diyl}{3-fluoro-2-[(2-ethylhexyl)carbonyl]thieno[3,4-b]thiophenediyl}) (PTB7).[12] The E_{HOMO} value for **P-BN-DPP** is very close to those of PTB7-Th and PTB7,[7,14] thus suggesting unfavorable photoinduced hole transfer. In view of the energy level alignments, **P-BN-IID** and **P-BN-TPD** can be used as polymer electron acceptors for all-PSCs.

All-PSC devices were fabricated using **P-BN-IID**/**P-BN-TPD** as the electron acceptor and PTB7-Th/PTB7 as the electron donor. The configuration of the device was ITO/PEDOT:PSS/active layer/Ca/Al. The active layer was spin-coated from a blend of polymer donor and polymer acceptor in *o*-DCB solution without any additive (see the Supporting Information). Figure 4 shows the *J-V* curves under AM 1.5G illumination (100 mW cm^{-2}) and the external quantum efficiency (EQE) spectra of the devices. The photovoltaic parameters are summarized in Table 2. The PTB7:**P-BN-IID** device has a PCE of 3.80 %, which is higher than that of the PTB7:**P-BN-TPD** device (PCE = 0.70 %). Whereas the PTB7-Th:**P-BN-TPD** device shows a low PCE of only 0.12 %, the device based on the PTB7-Th:**P-BN-IID** blend exhibits a much enhanced device performance with a PCE of 5.04 %, an open-circuit voltage (V_{oc}) of 0.92 V, a short-circuit

Table 2: Summary of the performance of the all-PSC devices.

Active layer	V_{oc} [V]	J_{sc} [mA cm^{-2}]	FF	PCE_{max} [%]	PCE_{ave}[a] [%]	EQE	μ_h [cm^2 V^{-1} s^{-1}]	μ_e [cm^2 V^{-1} s^{-1}]	μ_h/μ_e	α
PTB7-Th:**P-BN-IID**	0.92	11.37	0.48	5.04	4.95	0.53	1.88×10^{-4}	2.09×10^{-5}	9:1	0.97
PTB7:**P-BN-IID**	0.93	9.05	0.45	3.80	3.71	0.42	5.09×10^{-4}	1.41×10^{-5}	36:1	0.96
PTB7-Th:**P-BN-TPD**	1.08	0.51	0.22	0.12	0.10	0.15	2.66×10^{-6}	7.50×10^{-8}	35:1	0.92
PTB7:**P-BN-TPD**	1.00	2.48	0.30	0.70	0.63	0.03	1.25×10^{-4}	6.80×10^{-7}	181:1	0.91

[a] The average PCE value is calculated from eight devices.

current density (J_{sc}) of 11.37 mA cm^{-2}, and a fill factor (FF) of 0.48. This PCE is comparable to that of the best all-PSCs, which use polymer acceptors based on NDI or PDI units.[2–4] **P-BN-IID** with good all-PSC device performance represents a novel strategy to develop promising polymer acceptors based on the B←N unit. The four all-PSC devices all show broad EQE responses from 300 nm to 750 nm. The PTB7-Th:**P-BN-IID** blend has a maximum EQE of 0.53 and the PTB7:**P-BN-IID** blend shows a maximum EQE of 0.42. The calculated J_{sc} values from the integrations of the EQE spectra and the AM 1.5G spectrum agree well with the J_{sc} values obtained from the *J-V* curves, within an error of 5%.

The much higher J_{sc} and FF values of the devices based on **P-BN-IID** compared to those of **P-BN-TPD** are attributed mainly to the enhanced electron mobility of the polymer acceptor. The electron and hole mobilities of the four blends were evaluated using the SCLC method (Table 2). The electron mobility (μ_e) and hole mobility (μ_h) for the PTB7-Th:**P-BN-IID** blend are 2.09×10^{-5} cm^2 V^{-1} s^{-1} and 1.88×10^{-4} cm^2 V^{-1} s^{-1}, respectively. In comparison, the μ_e and μ_h values of the PTB7-Th:**P-BN-TPD** blend are 7.50×10^{-8} cm^2 V^{-1} s^{-1} and 2.66×10^{-6} cm^2 V^{-1} s^{-1}, respectively. The charge carrier mobilities are higher and more balanced for the PTB7-Th:**P-BN-IID** blend than for the PTB7-Th:**P-BN-TPD** blend. A similar trend is observed for the PTB7:**P-BN-IID** and PTB7:**P-BN-TPD** blends. We then studied the charge recombination in the all-PSC devices by measuring the dependence of the *J-V* characteristics on the light intensity. The J_{sc} value follows a power-law dependence on the illumination intensity ($J_{sc}\propto P_{light}{}^{\alpha}$), where P_{light} is the light intensity and α is the calculated power-law exponent. α should be unity when the bimolecular recombination is negligible.[2–4] Whereas the α value is 0.92 for the PTB7-Th:**P-BN-TPD** device and 0.91 for the PTB7:**P-BN-TPD** device, the α value is 0.97 for the PTB7-Th:**P-BN-IID** device and 0.96 for the PTB7:**P-BN-IID** device, respectively. The results clearly indicate that bimolecular charge recombination is efficiently suppressed in the **P-BN-IID**-based devices. The enhanced electron mobility of **P-BN-IID** leads to balanced charge transport and suppressed charge recombination in the active layer, and consequently results in the improved performance of the all-PSC device.

The nanoscale phase-separation morphology also plays an important role on the performance of the all-PSC device. The PTB7-Th:**P-BN-IID** blend shows a fibrillar nanostructure and fine phase-separated domains. In contrast, the PTB7-Th:**P-BN-TPD** blend exhibits a large-size phase-separation morphology without a fibrillar structure. These results are in accordance with the much better performance of the PTB7-Th:**P-BN-IID** device. A similar trend is also observed for the PTB7:**P-BN-IID** and PTB7:**P-BN-TPD** blends (Figure S9 shows the atomic force microscopy (AFM) topographical and phase images of the four active layers).

In summary, we have developed a series of promising polymer electron acceptors containing B←N units. By extending the length of the repeating units of the conjugated polymers, the effect of steric hindrance from the pendant phenyl groups is alleviated and the π–π stacking of the polymer backbones is promoted. The resulting polymer exhibits dramatically enhanced electron mobility and greatly improved all-PSC device performance. A PCE as high as 5.04% was demonstrated for all-PSCs using **P-BN-IID** as the electron acceptor. These results suggest that polymer electron acceptors with excellent all-PSC device performance can be developed from polymer electron donors by using B←N units.

Acknowledgements

We are grateful for financial support from the 973 Project (No. 2014CB643504), the Nature Science Foundation of China (No. 51373165, No. 21574129, No. 51325303, No. 21404099), the "Thousand Talents Program" of China, the Strategic Priority Research Program of the Chinese Academy of Sciences (No. XDB12010200), and the State Key Laboratory of Supramolecular Structure and Materials in Jilin University (No. sklssm201608).

Keywords: boron · conjugation · electron acceptor · polymers · solar cells

How to cite: *Angew. Chem. Int. Ed.* **2016**, *55*, 5313–5317
Angew. Chem. **2016**, *128*, 5399–5403

[1] a) T. Kim, J.-H. Kim, T. E. Kang, C. Lee, H. Kang, M. Shin, C. Wang, B. Ma, U. Jeong, T.-S. Kim, B. J. Kim, *Nat. Commun.* **2015**, *6*, 8547; b) A. Facchetti, *Mater. Today* **2013**, *16*, 123; c) G. Yu, J. Gao, J. C. Hummelen, F. Wudl, A. J. Heeger, *Science* **1995**, *270*, 1789.

[2] a) L. Gao, Z.-G. Zhang, L. Xue, J. Min, J. Zhang, Z. Wei, Y. Li, *Adv. Mater.* **2016**, *28*, 1884; b) C. Lee, H. Kang, W. Lee, T. Kim, K.-H. Kim, H. Y. Woo, C. Wang, B. J. Kim, *Adv. Mater.* **2015**, *27*, 2466; c) Y.-J. Hwang, B. A. E. Courtright, A. S. Ferreira, S. H. Tolbert, S. A. Jenekhe, *Adv. Mater.* **2015**, *27*, 4578; d) L. Ye, X. Jiao, M. Zhou, S Zhang, H. Yao, W. Zhao, A. Xia, H. Ade, J. Hou, *Adv. Mater.* **2015**, *27*, 6046; e) N. Zhou, H. Lin, S. J. Lou, X. Yu, P. Guo, E. F. Manley, S. Loser, P. Hartnett, H. Huang, M. R. Wasielewski, L. X. Chen, R. P. H. Chang, A. Facchetti, T. J. Marks, *Adv. Energy Mater.* **2014**, *4*, 1300785; f) C. Mu, P. Liu, W. Ma, K. Jiang, J. B. Zhao, K. Zhang, Z. H. Chen, Z. H. Wei, Y. Yi, J. N. Wang, S. H. Yang, F. Huang, A. Facchetti, H. Ade, H. Yan, *Adv. Mater.* **2014**, *26*, 7224; g) W. W. Li, W. S. C. Roelofs, M. Turbiez, M. M. Wienk, R. A. J. Janssen, *Adv. Mater.* **2014**, *26*, 3304; h) D. Mori, H. Benten, I. Okada, H. Ohkita, S. Ito, *Energy Environ. Sci.* **2014**, *7*, 2939; i) M. Schubert, B. A. Collins, H. Mangold, I. A. Howard, W. Schindler, K. Vandewal, S. Roland, J. Behrends, F. Kraffert, R. Steyrleuthner, Z. Chen, K. Fostiropoulos, R. Bittl, A. Salleo, A. Facchetti, F. Laquai, H. W. Ade, D. Neher, *Adv. Funct. Mater.* **2014**, *24*, 4068; j) M. Schubert, D. Dolfen, J. Frisch, S. Roland, R. Steyrleuthner, B. Stiller, Z. Chen, U. Scherf, N. Koch, A. Facchetti, D. Neher, *Adv. Energy Mater.* **2012**, *2*, 369.

[3] a) C. L. Chochos, N. Tagmatarchis, V. G. Gregoriou, *RSC Adv.* **2013**, *3*, 7160; b) X. Zhao, X. Zhan, *Chem. Soc. Rev.* **2011**, *40*, 3728; c) J. E. Anthony, A. Facchetti, M. Heeney, S. R. Marder, X. Zhan, *Adv. Mater.* **2010**, *22*, 3876.

[4] a) Y.-J. Hwang, T. Earmme, B. A. E. Courtright, F. N. Eberle, S. A. Jenekhe, *J. Am. Chem. Soc.* **2015**, *137*, 4424; b) H. Kang, M. A. Uddin, C. Lee, K.-H. Kim, T. L. Nguyen, W. Lee, Y. X. Li, C. Wang, H. Y. Woo, B. Kim, *J. Am. Chem. Soc.* **2015**, *137*, 2359; c) J. W. Jung, J. W. Jo, C.-C. Chueh, F. Liu, W. H. Jo, T. P. Russell, A. K.-Y. Jen, *Adv. Mater.* **2015**, *27*, 3310; d) T. Earmme, Y.-J.

Hwang, S. Subramaniyan, S. A. Jenekhe, *Adv. Mater.* **2014**, *26*, 6080; e) P. Cheng, L. Ye, X. Zhao, J. Hou, Y. Li, X. Zhan, *Energy Environ. Sci.* **2014**, *7*, 1351; f) Y. Zhou, T. Kurosawa, W. Ma, Y. Guo, L. Fang, K. Vandewal, Y. Diao, C. Wang, Q. Yan, J. Reinspach, J. Mei, A. L. Appleton, G. I. Koleilat, Y. Gao, S. C. B. Mannsfeld, A. Salleo, H. Ade, D. Zhao, Z. Bao, *Adv. Mater.* **2014**, *26*, 3767; g) I. H. Jung, W.-Y. Lo, J. Jang, W. Chen, D. L. Zhao, E. S. Landry, L. Y. Lu, D. V. Talapin, L. Yu, *Chem. Mater.* **2014**, *26*, 3450; h) E. J. Zhou, J. Z. Cong, K. Hashimoto, K. Tajima, *Adv. Mater.* **2013**, *25*, 6991; i) X. Zhan, Z. Tan, B. Domercq, Z. An, X. Zhang, S. Barlow, Y. Li, D. Zhu, B. Kippelen, S. R. Marder, *J. Am. Chem. Soc.* **2007**, *129*, 7246.

[5] a) L. Lu, T. Zheng, Q. Wu, A. M. Schneider, D. Zhao, L. Yu, *Chem. Rev.* **2015**, *115*, 12666; b) S. Zhang, L. Ye, W. Zhao, B. Tang, Q. Wang, J. Hou, *Sci. China Chem.* **2015**, *58*, 248; c) H. Song, H. Tong, Z. Xie, L. Wang, F. Wang, *Chin. J. Polym. Sci.* **2013**, *31*, 1117; d) Z. Lu, C. Li, C. Du, X. Gong, Z. Bo, *Chin. J. Polym. Sci.* **2013**, *31*, 901; e) Y. F. Li, *Acc. Chem. Res.* **2012**, *45*, 723; f) Y. J. Cheng, S. H. Yang, C. S. Hsu, *Chem. Rev.* **2009**, *109*, 5868; g) B. C. Thompson, J. M. J. Fréchet, *Angew. Chem. Int. Ed.* **2008**, *47*, 58; *Angew. Chem.* **2008**, *120*, 62.

[6] A. Wakamiya, T. Taniguchi, S. Yamaguchi, *Angew. Chem. Int. Ed.* **2006**, *45*, 3170; *Angew. Chem.* **2006**, *118*, 3242.

[7] C. Dou, Z. Ding, Z. Zhang, Z. Xie, J. Liu, L. Wang, *Angew. Chem. Int. Ed.* **2015**, *54*, 3648; *Angew. Chem.* **2015**, *127*, 3719.

[8] C. Dou, X. Long, Z. Ding, Z. Xie, J. Liu, L Wang, *Angew. Chem. Int. Ed.* **2016**, *55*, 1436; *Angew. Chem.* **2016**, *128*, 1458.

[9] a) Z. Zhang, H. Zhang, C. Jiao, K. Ye, H. Zhang, J. Zhang, Y. Wang, *Inorg. Chem.* **2015**, *54*, 2652; b) Z. Zhang, Z. Ding, C. Dou, J. Liu, L. Wang, *Polym. Chem.* **2015**, *6*, 8029; c) D. Frath, J. Massue, G. Ulrich, R. Ziessel, *Angew. Chem. Int. Ed.* **2014**, *53*, 2290; *Angew. Chem.* **2014**, *126*, 2322; d) D. Li, H. Zhang, Y. Wang, *Chem. Soc. Rev.* **2013**, *42*, 8416; e) P. Zalar, Z. B. Henson, G. C. Welch, G. C. Bazan, T.-Q. Nguyen, *Angew. Chem. Int. Ed.* **2012**, *51*, 7495; *Angew. Chem.* **2012**, *124*, 7613; f) K. Tanaka, Y. Chujo, *Macromol. Rapid Commun.* **2012**, *33*, 1235; g) Y.-L. Rao, S. Wang, *Inorg. Chem.* **2011**, *50*, 12263; h) F. Jäkle, *Chem. Rev.* **2010**, *110*, 3985; i) A. Job, A. Wakamiya, G. Kehr, G. Erker, S. Yamaguchi, *Org. Lett.* **2010**, *12*, 5470; j) M. J. D. Bosdet, W. E. Piers, T. S. Sorensen, M. Parvez, *Angew. Chem. Int. Ed.* **2007**, *46*, 4940; *Angew. Chem.* **2007**, *119*, 5028.

[10] a) X. Wang, J. Wang, J. Pei, *Chem. Eur. J.* **2015**, *21*, 3528; b) X. Wang, F. Zhuang, R. Wang, X. Wang, X. Cao, J. Wang, J. Pei, *J. Am. Chem. Soc.* **2014**, *136*, 3764; c) C. Dou, S. Saito, S. Yamaguchi, *J. Am. Chem. Soc.* **2013**, *135*, 9346; d) C. Dou, S. Saito, K. Matsuo, I. Hisaki, S. Yamaguchi, *Angew. Chem. Int. Ed.* **2012**, *51*, 12206; *Angew. Chem.* **2012**, *124*, 12372; e) C. D. Entwistle, T. B. Marder, *Angew. Chem. Int. Ed.* **2002**, *41*, 2927; *Angew. Chem.* **2002**, *114*, 3051.

[11] a) E. Wang, W. Mammo, M. R. Andersson, *Adv. Mater.* **2014**, *26*, 1801; b) Y. Deng, J. Liu, J. Wang, L. Liu, W. Li, H. Tian, X. Zhang, Z. Xie, Y. Geng, F. Wang, *Adv. Mater.* **2014**, *26*, 471; c) K. H. Hendriks, G. H. L. Heintages, V. S. Gevaerts, M. M. Wienk, R. A. J. Janssen, *Angew. Chem. Int. Ed.* **2013**, *52*, 8341; *Angew. Chem.* **2013**, *125*, 8499.

[12] a) S.-H. Liao, H.-J. Jhuo, Y.-S. Cheng, S.-A. Chen, *Adv. Mater.* **2013**, *25*, 4766; b) Z. He, C. Zhong, S. Su, M. Xu, H. Wu, Y. Cao, *Nat. Photonics* **2012**, *6*, 591.

[13] DFT calculations were performed using the Gaussian 09 program: M. J. Frisch, et al. Gaussian 09, revision A.02; Gaussian, Inc.: Wallingford, CT, **2009**. For details, see the Supporting Information.

[14] Z. Ding, Z. Miao, Z. Xie, J. Liu, *J. Mater. Chem. A* **2016**, *4*, 2413.

Received: February 4, 2016
Published online: March 17, 2016

